EvoDevo

RESEARCH

Open Access

Reinvestigating the early embryogenesis in the flatworm *Maritigrella crozieri* highlights the unique spiral cleavage program found in polyclad flatworms

Johannes Girstmair[1,2] and Maximilian J. Telford[1*]

Abstract

Background: Spiral cleavage is a conserved, early developmental mode found in several phyla of Lophotrochozoans resulting in highly diverse adult body plans. While the cleavage pattern has clearly been broadly conserved, it has also undergone many modifications in various taxa. The precise mechanisms of how different adaptations have altered the ancestral spiral cleavage pattern are an important ongoing evolutionary question, and adequately answering this question requires obtaining a broad developmental knowledge of different spirally cleaving taxa. In flatworms (Platyhelminthes), the spiral cleavage program has been lost or severely modified in most taxa. Polyclad flatworms, however, have retained the pattern up to the 32-cell stage. Here we study early embryogenesis of the cotylean polyclad flatworm *Maritigrella crozieri* to investigate how closely this species follows the canonical spiral cleavage pattern and to discover any potential deviations from it.

Results: Using live imaging recordings and 3D reconstructions of embryos, we give a detailed picture of the events that occur during spiral cleavage in *M. crozieri*. We suggest, contrary to previous observations, that the four-cell stage is a product of unequal cleavages. We show that that the formation of third and fourth micromere quartets is accompanied by strong blebbing events; blebbing also accompanies the formation of micromere 4d. We find an important deviation from the canonical pattern of cleavages with clear evidence that micromere 4d follows an atypical cleavage pattern, so far exclusively found in polyclad flatworms.

Conclusions: Our findings highlight that early development in *M. crozieri* deviates in several important aspects from the canonical spiral cleavage pattern. We suggest that some of our observations extend to polyclad flatworms in general as they have been described in both suborders of the Polycladida, the Cotylea and Acotylea.

Keywords: Blebbing, Evo-devo, Light-sheet microscopy, Live imaging, Polyclad flatworms, SPIM, Spiralians, Symmetry breaking, Turbellarians

*Correspondence: m.telford@ucl.ac.uk
[1] Centre for Life's Origins and Evolution, Department of Genetics, Evolution and Environment, University College London, London WC1E 6BT, UK
Full list of author information is available at the end of the article

Background

The Lophotrochozoa is one of two major clades of protostomes, sister group of the Ecdysozoa [1, 14, 23, 27, 59]. It contains approximately a dozen morphologically diverse and mostly marine phyla. While the adult morphology of the different phyla gives few obvious clues as to their close relationships, it has long been recognized that a subset of lophotrochozoan phyla share striking similarities in the earliest events of their embryology, most notably in the spatial arrangement of early blastomere divisions, a developmental mode known as spiral cleavage [26, 30, 40]. Representative lophotrochozoan phyla with spiral cleavage comprise annelids, molluscs, nemerteans, flatworms, phoronids and entoprocts [30, 40], and recent phylogenetic results show that these spirally cleaving phyla form a clade within the Lophotrochozoa [49]. The monophyly of the spirally cleaving phyla strongly suggests a single origin of the spiral cleavage mode. The fact that spiral cleavage has been maintained in these animals since they diverged in the early Cambrian, over half a billion years ago, argues that selection for maintaining spiral cleavage exists.

There are several aspects of spiral cleavage that appear to be highly conserved. The first is the spiral pattern itself: embryos of the eight-cell stage consist of four larger vegetal macromeres, 1Q, and four smaller animally positioned micromeres, 1q, each sitting skewed to one side of their sister macromere, above the macromeres' cleavage furrows. The typical spiral deformations (SD) of macromeres show a helical twist towards one side with respect to the animal–vegetal axis. This is best seen if the embryo is viewed from the animal pole. The resulting spiral shape taken by all four macromeres is either clockwise (dexiotropic) or counter clockwise (laeotropic). In subsequent rounds of division, the larger macromeres again divide unequally and asymmetrically, sequentially forming the second and then the third quartets of micromeres. During these divisions, the spiral deformations appear in alternating dexiotropic/laeotropic directions (the rule of alternation) up to the 64-cell stage. Polyclad flatworms follow this pattern up to the fifth cleavage where a 32-cell stage is reached. At this stage, eight cells of each quarter of the embryo can be traced back to one of the large cells at the four-cell stage and constitute the four quadrants, A, B, C and D. This stereotypical production of quartets means that individual blastomeres can be reliably recognized (and arguably therefore homologized) across spiralian phyla through development. To a variable extent, these homologous blastomeres have been shown subsequently to form lineages with similar fates across the Lophotrochozoa [32, 33, 47].

The four quadrants are sometimes individually identifiable as early as the four-cell stage and signify the embryo's future dorso-ventral axis and plane of bilateral symmetry. The D quadrant of spiralian embryos has received particular attention from comparative embryologists as there are two distinct mechanisms known for how the D quadrant is initially specified. Once determined, the D quadrant will give rise to micromere 4d. The 4d micromere contributes to endodermal structures (e.g. hindgut) but also becomes the sole source of the so-called endomesoderm, which emerges as two symmetrically distributed mesodermal bands. As micromere 4d produces endoderm and mesoderm, it is referred to as the "mesentoblast" [13, 38, 76, 78]. In snails, it has been shown that descendants of the D quadrant also possess organizer-like functions [11, 41, 51, 73]. The D quadrant lineage arguably holds some of the most conserved features found in spiral cleavers so far.

In addition to endomesoderm, which is derived from 4d, a second source of mesoderm (ectomesoderm) is known in spiralians. Ectomesoderm primarily gives rise to larval structures and has been shown in many species to originate from the second and third quartets of micromeres where it can derive from all four quadrants [33, 47].

While spiral cleavage is generally recognized as homologous and highly conserved across spiralian lophotrochozoans, there are, nevertheless, reports of variations on this conserved theme and even complete loss of this mode of development in different species. Alterations to the spiral cleavage mode include unusual arrangements and differences in relative sizes of blastomeres, alternative cell fates including rare derivations of the otherwise highly conserved origin of the mesoderm [55], and even complete loss of the spiral arrangements of blastomeres [26].

As mentioned before, endomesoderm arises predominantly from the D quadrant (but see [55]), but there are two different ways of specifying which of the four quadrants becomes the D quadrant. This crucial step can be achieved either early in development by producing blastomeres of different sizes (and presumably containing different maternal transcripts or proteins) or by a later inductive event. Embryos with different sized blastomeres are classified as "unequal cleavers" whereby the D blastomere at the four-cell stage is typically the largest cell [16, 42]. There are clearly different mechanisms in how the unequal cleavers determine the D quadrant. Some have polar lobes (cytoplasmic eversions that can move determinant material to specific blastomeres during the first and second cleavages), others show asymmetric positioning of the spindle during cleavage, yet others destroy one of the centrosomes [64]. In species using induction (equal cleavers), D quadrant specification is thought to take place by an interaction between

cells, usually between one of the large macromeres and the first quartet of micromeres (see [47]). In the latter case, the specification of the D quadrant occurs later in development, with some significant variations in timing. Furthermore, in some special cases slight size differences alone can bias the fate of one blastomere toward "D" in equal cleavers [16].

To reconstruct the ancestral features of spiral cleavage and to further the understanding of the adaptive basis of any modifications of the spiral cleavage program, it is essential to broaden our knowledge of the phylogenetically conserved and variable features of the spiral cleavage program by studying the full diversity of spiral cleavers. Here we focus on both the conserved and the derived aspects of early spiral cleavage in one important but understudied lophotrochozoan phylum: the Platyhelminthes (flatworms). Across the Platyhelminthes, a wide range of different evolutionary developmental modes is found, indeed, in most members of the phylum spiral cleavage has been lost entirely. Only the Polycladida and its sister group, the Prorhynchida [15, 50] have retained an apparently canonical form of spiral cleavage including the formation of several quartets. For this reason, both taxa are excellent candidates for evolutionary comparative studies [44, 50]. Other flatworms have only partially retained spiral cleavage (e.g. *Macrostomum lignano* [57, 81]).

The development of polyclad flatworms closely follows the conserved spiral cleavage mode and this is true of both polyclad suborders, the Acotylea and Cotylea, as well as in direct and in indirect developers within both suborders [7, 18, 21, 35, 43, 44, 48, 50, 61, 71, 82]. Cleavage in polyclads, as in other spiralians, begins with two meridional divisions (from animal pole to vegetal pole) resulting in four cells arranged around the central animal–vegetal axis and these blastomeres are given standard names of A, B, C, D. The stereotypical polyclad cleavage pattern after the four-cell stage from the third to the fifth cleavage (32-cell stage) is summarized in Fig. 1a–c. Three quartets of ectodermal micromeres (1q–3q) are budded at the animal pole by repeated divisions of the large macromeres. In most spiral cleavers, a fourth and sometimes even a fifth quartet of blastomeres are formed in this specific geometry. In polyclad flatworms, however, the fourth quartet deviates significantly from the stereotypic cleavage in terms of both relative size of micromeres and macromeres and their orientation. In contrast to the formation of the first three quartets of micromeres, the fourth quartet 'micromeres' are considerably larger than the four sister 'macromeres' which form as four small cells at the vegetal pole (see Fig. 1d). This unusual characteristic of large fourth quartet micromeres has previously been observed in polyclad flatworms including both *H. inquilina* [7] and *M. crozieri* [61].

Most of our current knowledge of polyclad embryogenesis derives from observations made in embryos of *Hoploplana inquilina* [7, 71], which belongs to the Acotylea, one of the two major suborders found within polyclad flatworms [43]. Here, we investigate the early cleavages of *Maritigrella crozieri* a member of the Cotylea—the second major clade of polyclads. *M. crozieri* has recently been introduced as a model to study flatworm evolution and development [20, 44, 61]. Here we provide the most detailed description to date of the early development of a cotylean polyclad flatworm. To visualize the development of embryos in vivo we used a recently established live imaging set-up, using selective plane illumination microscopy (SPIM) via the OpenSPIMopen access platform [22, 60], which allows in vivo recordings and precise 3D reconstructions of polyclad flatworm embryos [20]. We use 4D live imaging to visualize details of the early development of *M. crozieri*, and we examine cell volume measurements of blastomeres from the first and second cleavages. Live imaging has also allowed us to make new observations of cell shape deformations in blastomeres during early cleavage.

Results and discussion

Live imaging observations of spiral cleavage in *Maritigrella crozieri*

Our observations of *M. crozieri's* earliest cleavage pattern, which include live imaging recordings (Fig. 2) and scanning electron microscopy images (Fig. 3a–f) are in accordance with previous 4D recordings up to the 16-cell stage [44] and descriptions of fixed specimens [61]. In some specimens, we noted that second cleavages were slightly asynchronous, which explains the occasional observation of embryos in a three-cell stage before the formation of four similarly sized blastomeres takes place. The characteristic cleavage pattern and spiral deformations are prominent; the four-cell to eight-cell transition is dexiotropic (compare Fig. 1a, Fig. 3a and Additional file 1). As the division of the first quartet micromeres (1a–1d) is slightly delayed relative to the division of their sister macromeres (1A–1D), an intermediate 12-cell stage forms (Fig. 3c, d). During the generation of new quartets by divisions of macromeres, the micromeres of the existing quartets also divide and, after the third quartet is completed, the embryo reaches a 32-cell stage. Up to this point, the cleavage appears symmetric, and we could not observe any signs that this symmetry is broken, as is often the case in unequal cleavers.

In developing polyclads, including *M. crozieri* [61], it is known that, during the polyclad-specific fourth quartet formation (the unusual asymmetric division resulting in

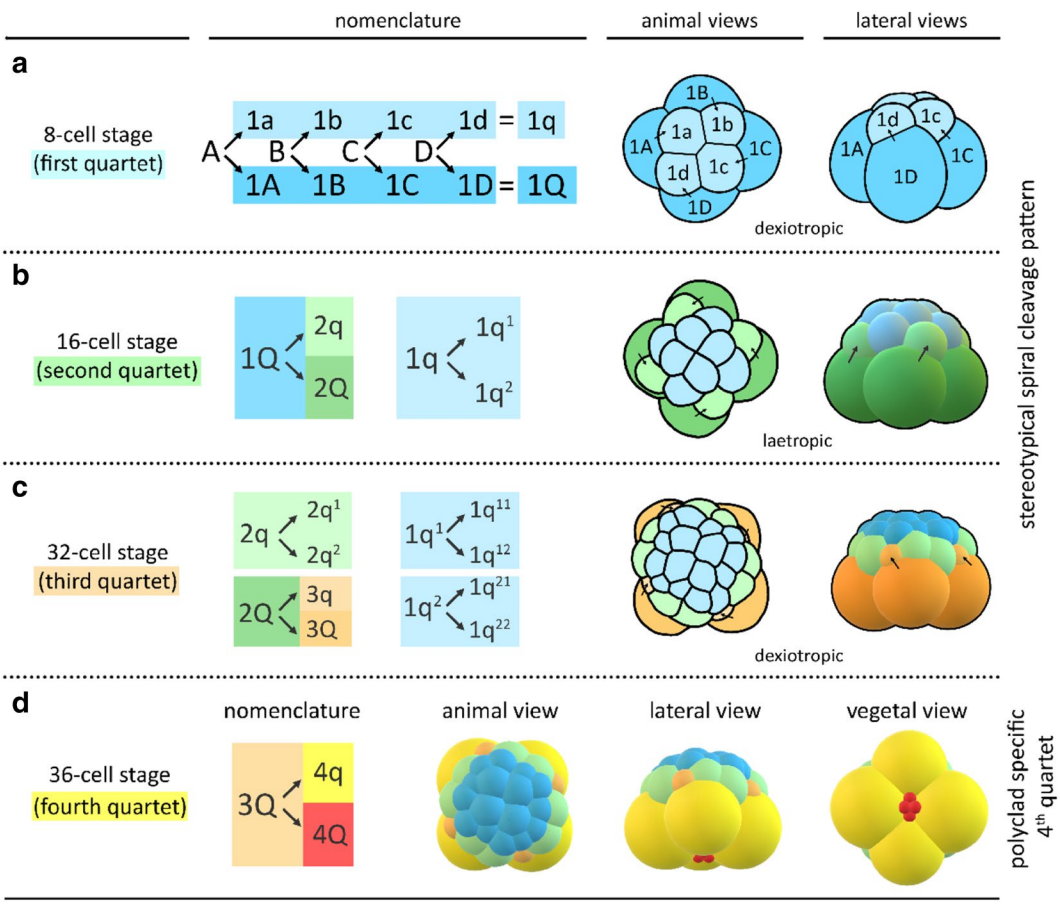

Fig. 1 Schematics and nomenclature of the spiral quartet cleavage as found in polyclad flatworms. Micromere and macromere quartets (q and Q, respectively) are colour-coded. **a** The third cleavage (four- to eight-cell stage) is unequal and asymmetric. The eight-cell stage embryo consists of four larger vegetal macromeres 1Q, and four smaller animally positioned micromeres 1q sitting skewed to one side of their sister macromere, above the macromeres' cleavage furrows. The typical spiral deformations (SD) of macromeres show a helical twist towards one side with respect to the animal–vegetal axis. This is best seen if the embryo is viewed from the animal pole. The resulting spiral shape taken by all four macromeres has been shown to be either clockwise (dexiotropic) or counter clockwise (laeotropic) among different lophotrochozoans. In the polyclad *M. crozieri* it is dexiotropic. Notably it has been demonstrated that the mechanism of spiral deformations depends on actin filaments rather than on spindle forming microtubules [70]. **b**, **c** In subsequent rounds of division, the larger macromeres again divide unequally and asymmetrically sequentially forming the second and then the third quartets of micromeres. During these divisions the spiral deformations appear in alternating dexiotropic/laeotropic directions (the rule of alternation). Up to the 32-cell stage, polyclad flatworms represent a classic example of stereotypic lophotrochozoan spiral quartet cleavage. **d** The formation of the fourth quartet (4Q and 4q) deviates from the typical pattern seen in other spiral-cleaving embryos insofar as the micromeres 4q become large and the macromeres 4Q diminutive. Q = A, B, C, D; q = a, b, c, d

large micromeres and small fourth quartet macromeres), a significant displacement of the nuclei in all four macromeres (3Q) occurs prior to their division. This is shown here in embryos of *M. crozieri* using live imaging recordings and 3D reconstructions (Fig. 3i–l). The macromere nuclei, which are typically placed towards the animal pole, shift significantly towards the vegetal pole in 3A–3D (Fig. 3g, h, blue arrows). As a result of these movements, the nuclei of 3A–3D meet at the vegetal pole of the embryo, just before the macromeres divide (Fig. 3k, purple nuclei). The newly formed large micromeres retain most of their size and all the yolk. After the completion of the fourth quartet of micromeres, embryos have reached the 36-cell stage. In polyclads, except for micromere 4d, cells of the fourth quartet do not appear to undergo any further divisions for as long as they can be traced during epibolic gastrulation [7, 61, 71]. At the point when cilia form on the epidermis and embryos start to rotate, cells become difficult to identify and their fates obscure. However, before rotation starts, there is evidence from our live imaging recordings that, during epiboly and after bilateral symmetry is established, these small macromeres could engage in further cell–cell interactions. The nuclei of the small macromeres (4A–4D) can be

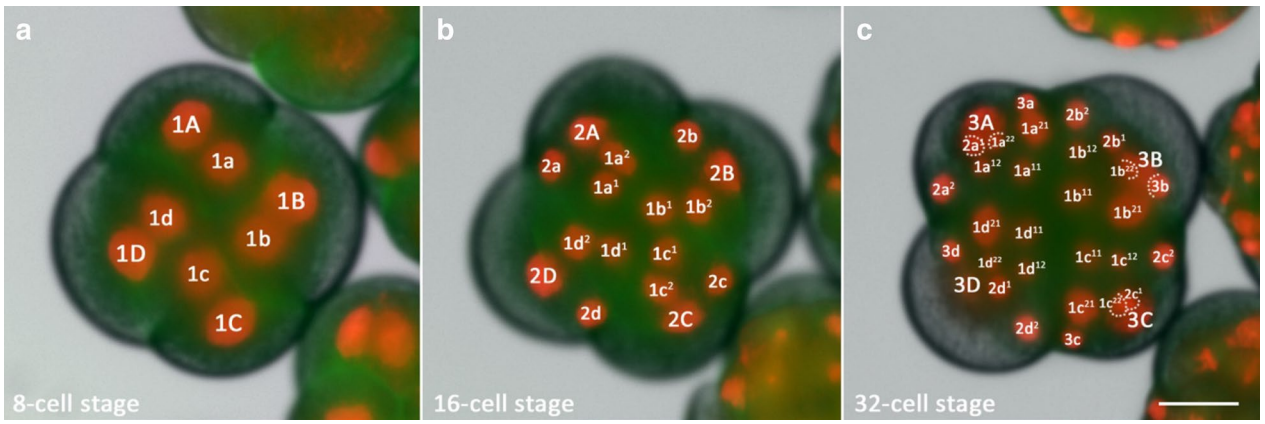

Fig. 2 Live imaging of the transition from an8-cell stage embryo to a 32-cell stage in *M. crozieri* with nuclei labelled according to the canonical spiral cleavage nomenclature. **a** The eight-cell stage is a product of a dexiotropic cleavage. **b** The 16-cell stage with its first quartet micromeres (after their first cleavage round) and second quartet micromeres (2a–2d) and macromeres (2A–2D). **c** The embryo has now reached the 32-cell stage. Images captured with a Zeiss Axio Zoom.V16 Stereo Microscope. Scale bar is 50 µm

seen in close proximity with nuclei of descendants of micromere $4d^1$ (probably micromere $4d^{11}$) as is shown in Fig. 4 and as a movie (see Additional file 2). While this observation alone does not tell us whether the "interaction" of a migrating cell has any further significance for the embryo, we suggest that the fourth quartet macromeres, despite their early cell division arrest, could still play a more important developmental role during gastrulation than has previously been appreciated.

The dramatic changes from an animally positioned cleavage position to a vegetal one resulting in small fourth quartet 'macromeres' (4A–4D) are not observed in most other spirally cleaving embryos. This deviation from the typical quartet formation pattern raises the question as to how and why such a modification evolved. Unusual size differences of blastomeres during early cleavages have been described several times in other spiralians, in nemerteans [17] and sipunculids [67], for example, where larger micromeres correlate with an enlarged episphere of the developing larvae. In polyclads, one possible explanation for the unusual behaviour of the fourth quartet macromeres is that the secondary loss of the anus in flatworms might have altered the spiral cleavage pattern. The blastomeres, which initially contributed to endodermal structures of the through-gut, would have become redundant and—in the case of polyclads—significantly decreased in size and are now assumed to degenerate during development (see [44]). This view is supported by the fact that the fourth quartet macromeres (4A–4D) give rise to endodermal structures in other spiralians. Interestingly, in the common bladder snail *Physa fontinalis*, the fourth quartet emerges in a very similar way to polyclad flatworms, producing a rosette of four smaller macromeres (4A–4D) at the most vegetal pole and four larger micromeres (4a–4d) above it [80]. In *P. fontinalis*, unlike polyclad flatworms, macromere 3D divides significantly earlier than its sister cells (3A–3C) giving rise to micromere 4d (the mesentoblast). Furthermore, in *P. fontinalis*, cells of the small macromere rosette (4A–4D) undergo a further division producing a fifth quartet of micromeres through equal divisions of 4A–4C.

The four-cell stage is a product of asymmetric cleavages in *M. crozieri*

In many spiral cleavers, equal and unequal cleavage types can be distinguished during the first two divisions. The cleavage mode has been thought to reflect the way in which the embryo determines one of its four quadrants to become designated as the D quadrant [3, 52, 74, 75]. As the D quadrant plays a major developmental role in the developing embryo, we wanted to measure the relative sizes of blastomeres in *M. crozieri*, in particular, after the second cleavage takes place. Polyclad flatworms, including *M. crozieri*, have been considered equal cleavers on the basis of their indistinguishable relative blastomere sizes at the two- and four-cell stages [44, 50, 61]; however, slight size differences at four-cell stages have been reported several times in polyclad flatworms [2, 35, 71, 72]. To test this in *M. crozieri*, we performed a series of precise blastomere volume measurements during the first and second cleavages. We 3D reconstructed 25 fixed embryos between the two- and four-cell stages. Additional file 3 (A–E and A′–E′) depicts how the precise volume of given blastomeres can be measured manually using an open source Fiji-plugin (Volumest; http://lepo.it.da.ut.ee/~markkom/volumest/). The measurement

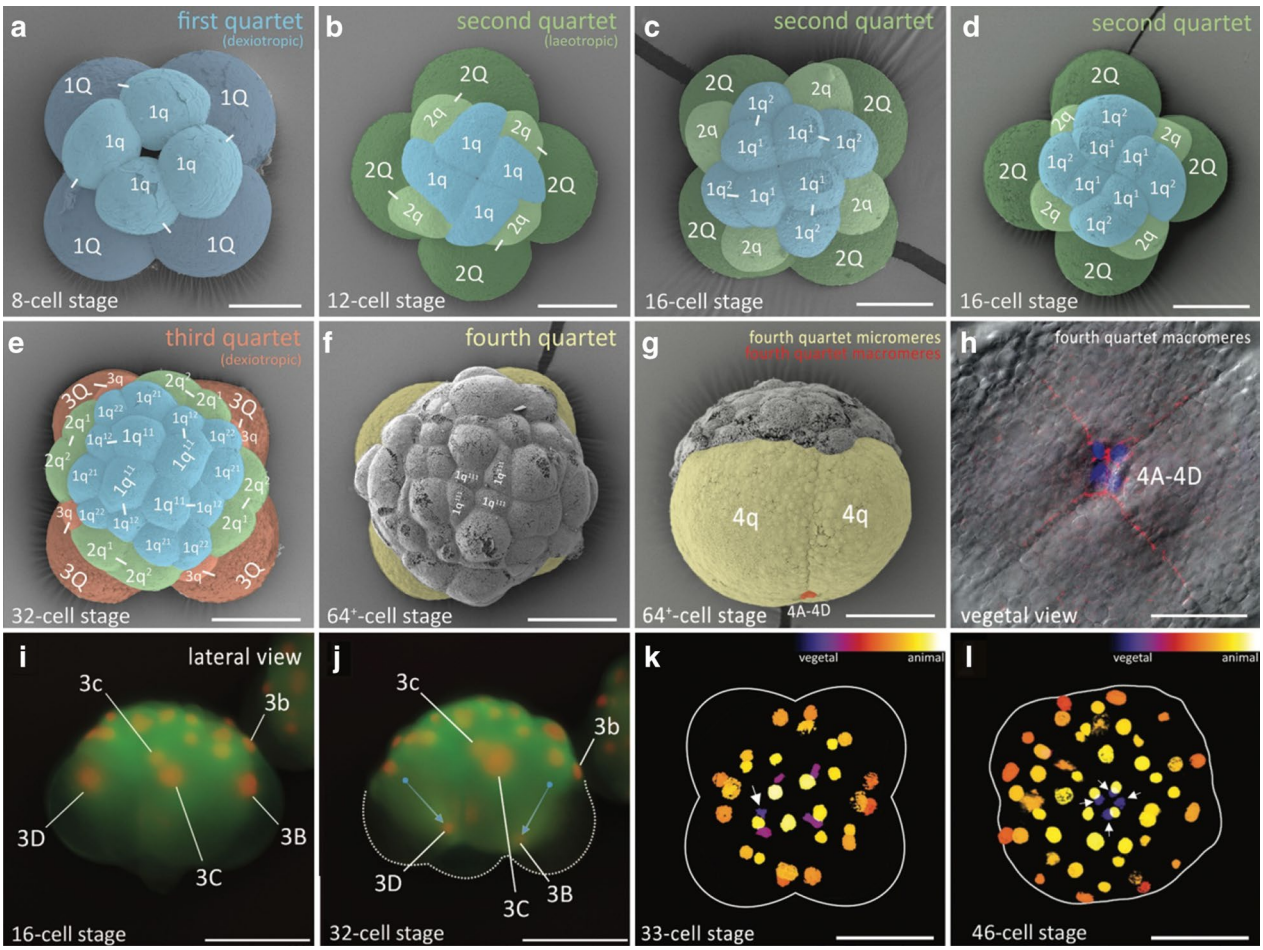

Fig. 3 Formation of the four quartets in *M. crozieri*. **a**–**g** SEM pictures coloured according to micromere quartets. **a** First quartet (1Q and 1q indicated in blue). **b**–**d** Second quartet (2Q and 2q) indicated in green. **e** Third quartet (3Q and 3q) indicated in orange. **f**, **g** The large fourth micromere quartet (4q) are shown and indicated in yellow. The fourth quartet micromeres are shown in red. **h** Closeup of the fourth quartet micromeres (4A–4D) with Phalloidin staining (red) outlining their cell shape. Nuclear staining (blue) is DAPI. **i**–**l** Formation of the fourth quartet. **i** The 16-cell stage shows macromeres 3B-D and their nuclei at an animal position within the large blastomeres. **j** Same embryo as in G but at the 32-cell stage. Nuclei of 3B and 3D are now positioned at the vegetal pole of the macromeres. **k** 33-cell stage of a 3D reconstructed embryo (Their depth in the embryo is coded by colours as seen in top right part of the panel. Division of one of the four macromeres (3Q) into 4Q/4q has taken place. The white arrow indicates the newly formed small macromere of the fourth quartet (4Q) coloured purple indicating it is close to the vegetal pole. **l** 3D reconstructions showing that all four macromeres comprising the fourth quartet are now positioned at the most vegetal pole of the embryo (coloured purple and indicated by arrows). Scale bar sare 50 µm

data of individual blastomeres can be seen in Additional file 4. For convenience and easier comparison, we labelled vegetal cross-furrow cells in *M. crozieri* as B and D of which the larger cell was always designated as D. Accordingly, the remaining cells were labelled as A and C in consideration of the dextral cleavage type present in *M. crozieri*. One should keep in mind that this assignment may not represent the true quadrants [62], but this process allows us to see at least whether there is a consistently larger blastomere and, if so, whether this is an animal or vegetal cross-furrow cell.

A small but consistent volume difference of 6% (± 1.6%) on average could be discerned between the two blastomeres at the two-cell stage ($n = 13$) (Fig. 5f and Additional file 4). Two embryos of a transient three-cell stage show that volumes of the two sister cells also differ (Fig. 5g and Additional file 5) and together have a larger volume than the remaining third blastomere. In the four-cell stages, in 9/10 cases, the vegetal cross-furrows of the reconstructed embryos were clearly identifiable as schematically drawn in Fig. 5b and depicted in Fig. 5f, f′. Measuring individual blastomeres of four-cell stage embryos ($n = 10$) indicates that one of the four

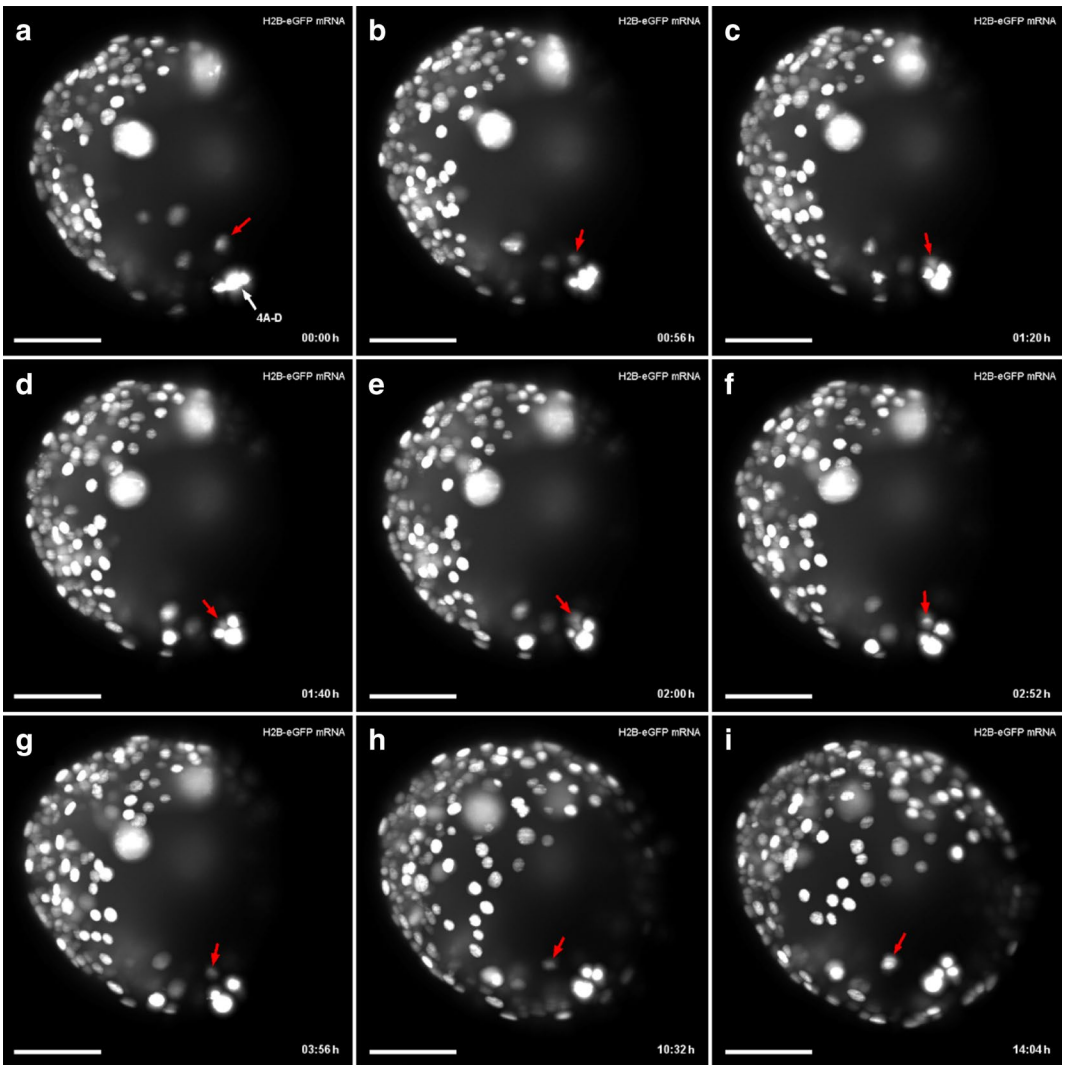

Fig. 4 Putative cell–cell interactions observed in the gastrulating polyclad flatworm *M. crozieri*. **a**–**i** A descendant of cell 4d[1] (red arrow) is traced and can be seen approaching and later departing from fourth quartet macromeres 4A-D before epiboly is completed. Time represents hours (h) of time-lapse imaging with an OpenSPIM. Scale bars are50 µm

cells is larger than the others (Fig. 5e and Additional file 5). Additionally, whenever vegetal cross-furrows of four-cell stage embryos are recognizable, the cell with the largest volume can be identified as one of these. Based on these measurements, *M. crozieri* undergoes asymmetric cell divisions during the first and second cleavages, although they are more pronounced during the two- to four-cell transition.

Understanding whether a spiralian embryo is an unequal or equal cleaver is important as it has major implications for determining the mechanism of D quadrant specification. In unequal cleavers (with unequal sized blastomeres at the four-cell stage), the D quadrant can be determined as early as the four-cell stage: it is assumed that a differential distribution of maternal factors takes place during the first two divisions coinciding with a noticeable inequality of the size of the large D blastomere in comparison with blastomeres A–C [4, 9, 10, 13, 28, 29, 31, 65, 66].

D quadrant specification in equal cleavers requires an inductive interaction, usually between one of the equal sized, large vegetal macromeres and the first quartet of micromeres positioned at the animal pole [76].

So far, *H. inquilina* is the only polyclad flatworm where blastomere deletion experiments have indicated that, in two-cell and four-cell stage embryos, asymmetrically distributed morphogenetic determinants could be involved in development [5] as expected of an unequal

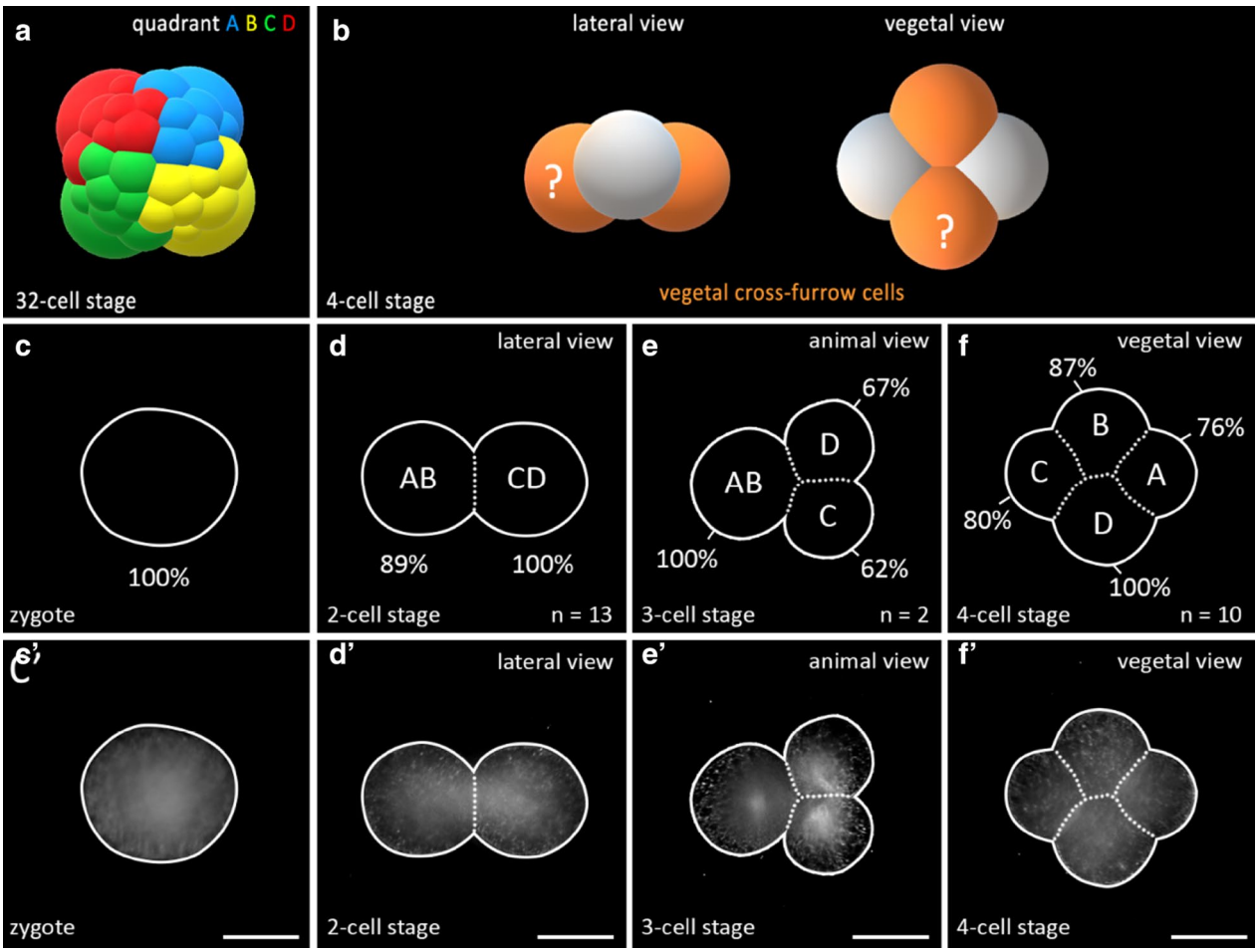

Fig. 5 Averaged volume measurements in *M. crozieri* blastomeres of the first and second cleavages. **a** A 3D model of a 32-cell stage embryo is shown with descendants derived from the same four-cell blastomere indicated by the same colour. **b** A 3D model of a four-cell stage embryo is depicted showing both vegetal cross-furrow cells that meet at the vegetal pole indicated in orange. Whether the D quadrant is already specified in *M. crozieri* at the four-cell stage remains unclear, which is indicated here by a question mark. **c**–**f** Volumes are given as a percentage of the volume of the total embryo, which is 100% (A). **d** At the two-cell stage the larger cell is assumed to represent blastomere CD and the smaller cell blastomere AB. **e** At the three-cell stage division of blastomere CD most likely precedes the division of blastomere AB. **f** At the four-cell stage the largest blastomere is always one of the vegetal cross-furrow cells and is interpreted as the D blastomere. **c′**–**f′** All volume measurements come from five-angle 3D multiview reconstructions and have been orientated with a view from their vegetal side. Only a single plane of the 3D reconstructed stack is shown. Scale bar = 100 µm

cleaver. In the unequally cleaving snail *Ilyanassa obsolete*, a mechanism for asymmetric messenger RNA segregation by centrosomal localization during cleavage has been described [39], and it would be interesting to test for a similar molecular mechanism in polyclad flatworms and to screen for components that play a crucial role in asymmetric cell division machinery as has been recently performed in the spiral-cleaving embryo *Platynereis dumerilii* via RNA sequencing [58]. There is, however, also evidence for cell–cell interactions between macromeres and micromeres in *H. inquilina* as is typical of equal cleavers [6].

While our volume measurements suggest that *M. crozieri* does not follow a strictly equal cleavage pattern, it would be premature to conclude that an unequal mechanism for D quadrant specification occurs. The differences we observe in blastomere sizes are relatively subtle and could be partly caused by natural variation. Natural variation in blastomere size can occur in equal cleavers, as has been reported for example in the nemertean *Carinoma tremaphoros* during the third cleavage [53] or in the pond snail *Lymnaea stagnalis* during their first two cleavages. For *L. stagnalis*, it was suggested that these naturally occurring size differences at the four-cell stage

lead to the emergence of vegetal cross-furrow cells as a consequence of more stable cell-packing arrangements. Thereby the larger cells tend to take a more vegetal position, become more centralized and thus have a higher probability of engaging in inductive interactions and hence D quadrant specification (see, e.g. [16]). It has been demonstrated experimentally that artificially enlarging one of the cells biases this blastomere towards acquiring D quadrant specification [16]. In *M. crozieri*, the presence of vegetal cross-furrow cells are also notable and may be the result of slightly oblique spindle orientations that have been observed in polyclads during the second cleavage [43, 71]. In this case, vegetal cross-furrow cells would form regardless of differences in blastomere size. Nonetheless, cell-packing arrangements similar to the four-cell stage of *Lymnaea* may be involved, and it would be reasonable to assume that a similar mechanism for acquiring D quadrant specification might be taking place in both species. Additionally, in unequal cleavers, where the D quadrant is specified at a very early stage, the symmetry is often broken prior to the fifth cleavage. As we do not observe this in *M. crozieri*, this could be interpreted as another indication for an equal cleavage mechanism.

Taken together, while our volume measurements alone cannot resolve the question of whether an equal or unequal cleavage mechanism takes place in *M. crozieri*, it is apparent that asymmetric cleavages do take place. It would be valuable to conduct precise volume measurements in other apparently equal cleaving spiralians, to determine whether they display any subtle biases (e.g. larger vegetal cross-furrow cells) that have gone undetected.

Micromere 4d in *M. crozieri* shows a cleavage pattern unique to polyclad flatworms

In embryos with spiral cleavage, micromere 4d typically divides into a left and a right daughter cell by a meridional division. It is at this point that the bilateral symmetry of the embryo first emerges at a cellular level. To determine the symmetry-breaking event during *M. crozieri* development, we followed the division pattern of micromere 4d using our live imaging data. We observe that the 4d blastomere in *M. crozieri* does not divide meridionally into a left and right daughter cell, but first divides along the animal–vegetal axis into a smaller, animally positioned cell, which we designate as $4d^2$ and a larger, vegetally positioned cell, we designate $4d^1$ (Fig. 6a, b, f, h; Additional file 6). We thereby follow closely the nomenclature used by Surface [71], and it should be noted that in this specific case (the animal–vegetal division of an ento- and mesoblast and not the ectoblast) the smaller exponent was intentionally reserved for the more

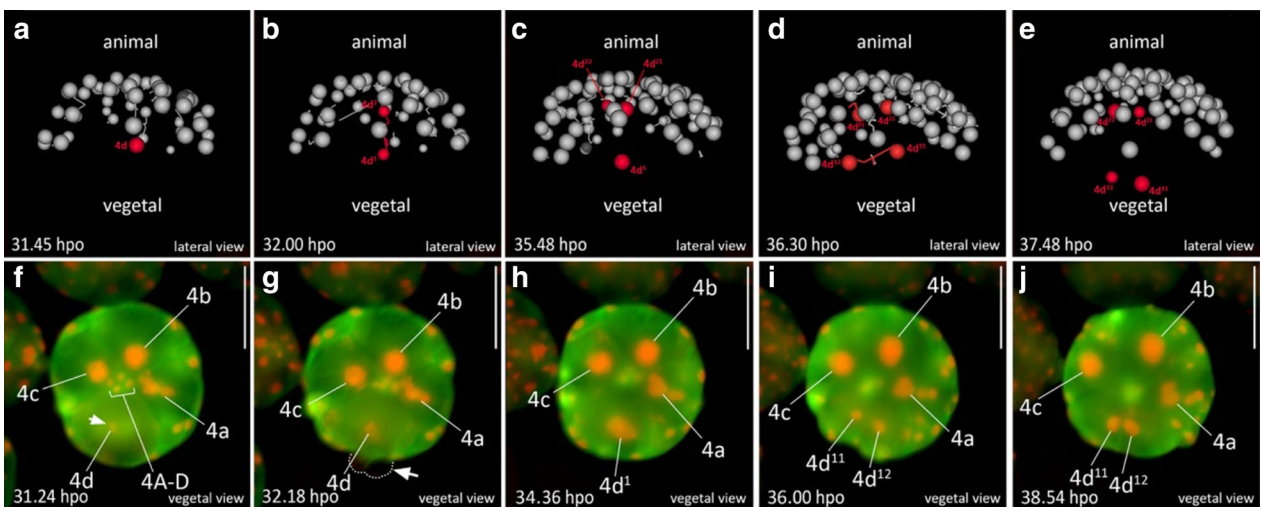

Fig. 6 Animal view of the cleavages of micromere 4d in *M. crozieri*. **a**–**e** The cleavage pattern of micromere 4d (marked in red) is visualized using a 3D viewer (Fiji), showing in grey the position of all remaining nuclei except 4A-D and 4a–4c. **a** Micromere 4d before its division. **b** Micromere 4d divides along the animal–vegetal pole and daughter cell $4d^2$ is budded into the interior of the embryo and in close proximity to micromeres of the animal pole. **c**–**e** Both daughter cells of micromere 4d divide again, but this time both cells cleave meridionally. **f** Micromere 4d undergoes mitosis revealing the D quadrant. **g** The asymmetric division of micromere 4d along the animal–vegetal pole is barely visible but causes blebbing (arrow pointing at dashed line). **h** After the division, daughter cell $4d^1$ remains large and is more vegetally positioned and therefore readily visible. $4d^2$ is budded into the interior of the embryo, more animally positioned and cannot be seen anymore without optical sectioning. **i**, **j** Bilateral symmetry is clearly visible after the division of $4d^1$. Oocytes were microinjected with nuclear marker H2A-mCherry (red) and microtubule marker EMTB-3xGFP (green) and the embryo used for 4d microscopy with OpenSPIM (A-E) or under a Zeiss Axio Zoom.V16 Stereo Microscope (F-J); hpo = hours post oviposition. Scalebar in images captured with the Axio Zoom = 100 µm

vegetally positioned "parent" cell. Only following this additional division of micromere 4d is definitive bilateral symmetry established by the meridional (left–right) division of both sister cells, $4d^1$ and $4d^2$ (Fig. 6c–e, h–j). The meridional divisions of $4d^1$ and $4d^2$ appear equal and this equality is easily observed in $4d^2$ due to its larger size and exposed external position. Both descendants of $4d^1$ and $4d^2$ ($4d^{11}$ and $4d^{12}$ and $4d^{21}$ and $4d^{22}$) then undergo another round of roughly meridional cleavages. This is similar to Surface's descriptions in *H. inquilina* [71].

Surface [71] and later van den Biggelaar [74] both already noted that in polyclads the cleavage of 4d differs from the canonical pattern of an immediate, equal and meridional division into left and right descendants. According to van den Biggelaar, in the polyclads *Hoploplana inquilina* and *Prostheceraeus giesbrechtii*, this meridional division is delayed by one cell cycle as 4d first undergoes the approximately animal–vegetal division into $4d^1$ and $4d^2$. This is followed by meridional cleavages of both daughter cells $4d^1$ and $4d^2$. These observations exactly match what we observe in *M. crozieri*. In other more recent descriptions of polyclad flatworms [25, 48, 61, 72, 83], this animal–vegetal division of 4d is not mentioned suggesting either that some polyclad flatworms lack it or, more likely, that the division is difficult to observe without continuous recording. Our observations in the *M. crozieri,* together with description of *H. inquilina* by Surface and *P. giesbrechtii* by van den Biggelaar strongly suggests that this cleavage pattern of micromere 4d is in fact unique among spiralians but common across polyclads.

Post-meiotic protrusions of the cell membrane (blebbing) accompany early development in *M. crozieri*

In several animal phyla, oocytes undergo cytoplasmic changes that are capable of temporarily deforming the shape of the egg and which have been suggested as a sign of the oocyte segregating cell content [79]. Such events have been commonly observed during fertilization and meiosis [12, 34, 45, 46, 54]. In polyclads, this has been demonstrated many times previously and is referred to as cell blebbing [2, 18, 21, 24, 35, 48, 63, 69, 71, 72, 83]. It has occasionally been noted that cell blebbing is not restricted to egg maturation and the extrusion of the polar bodies but can reappear frequently during early cleavages [19, 48, 72].

In *M. crozieri*, our observations show that blebbing during egg maturation follows first a depression of the oocyte at the animal pole (Fig. 7a) followed by protrusions all over the cell membrane (Fig. 7c and insets). These events are almost identical to drawings of egg maturation and oocyte blebbing based on different Japanese polyclad species by Kato [35].

Blebbing in *M. crozieri* continues after meiosis, specifically during the asymmetric cleavages of macromeres (Fig. 7). The formation of the third and fourth quartet micromeres is clearly accompanied by strong blebbing events in the macromeres distinct from what is seen in meiotic cell blebbing (Fig. 7e–l). In the case of the third quartet formation, we observe that, prior to the cleavage of macromeres 2A–2D, blebbing becomes visible on their cell surfaces in form of small, vesicle-like protrusions (Fig. 7e–h) ($n = 17/18$). The role of these vesicles is not clear, but we can observe that mitotic cytoskeletal activity during anaphase correlates with the observed protrusions (Additional files 7 and 8). In contrast, during the formation of the fourth quartet (3A–3D), cytoplasmic perturbations create waves of contractile activity with smaller blebs that appear more frequently. In this case, the macromeres can sometimes attain an elongated shape (Fig. 7i–l) ($n = 18/18$) at the onset of the formation of micromeres 4a–4d. More detailed time-lapse sequences of these peculiar cytoplasmic perturbations are shown in Additional file 9. Finally, the asymmetric division of micromere 4d in *M. crozieri* is also accompanied by distinctive cytoplasmic perturbations of the membrane

(See figure on next page.)

Fig. 7 Blebbing events during meiosis and spiral cleavage in the polyclad flatworm *M. crozieri*. **a**–**d** Blebbing during egg maturation in *M. crozieri* oocytes. **a** Extrusion of first polar body (white arrow) and depression of the oocyte at the animal pole (black arrowhead). **b** Oocyte with one polar body and darkish pigment accumulated at the animal pole. **c** Cell blebbing is recognizable by the formation of amoeboid/pseudopodia-like irregularities all over the cell membrane. **d** An egg cell is shown with two polar bodies and darkish pigment accumulated at the animal pole. **e**–**l** Blebbing is depicted during the third and fourth quartet formation. **e**–**h** Peculiar protrusions, which appear prior to third quartet formation (16–32-cell stage) among all four macromeres are shown. **i**, **j** Vegetal (**i**) and lateral view (**j**) of the division of macromere 3D into tiny macromere 4D (white arrowhead). **k**, **l** Blebbing is accompanied by severe deformations of large micromeres 4b and 4d. **m**–**p** Animal view of the cleavages of micromere 4d in *M. crozieri*. **m** Chromosome condensations are only visible in 4d. **n** Division of 4d is visible along the animal–vegetal axis of the embryo. White arrowheads show cytoplasmic perturbations during the cleavage of micromere 4d. **o** The meridional division of $4d^1$ takes place. **p** The next division of the daughter cells of $4d^1$ is depicted. **m′**–**p′** The 4d cell and its progenies have been depicted separately below at increased exposure levels. Embryos with fluorescent signal were microinjected as oocytes with a microtubule marker (EMTB-3xGFP) and a histone nuclear marker (H2A-mCh). Live imaging was performed under a Leica DMI3000 B inverted scope (**a**–**g**), a Zeiss Axio Zoom.V16 Stereo Microscope (**h**–**l**) and an OpenSPIM (**m**–**p**). Scalebar is 100 µm in **a** and **h**, 50 µm in I-L, 100 µm in **a** and **e** and 50 µm in **m**–**p**

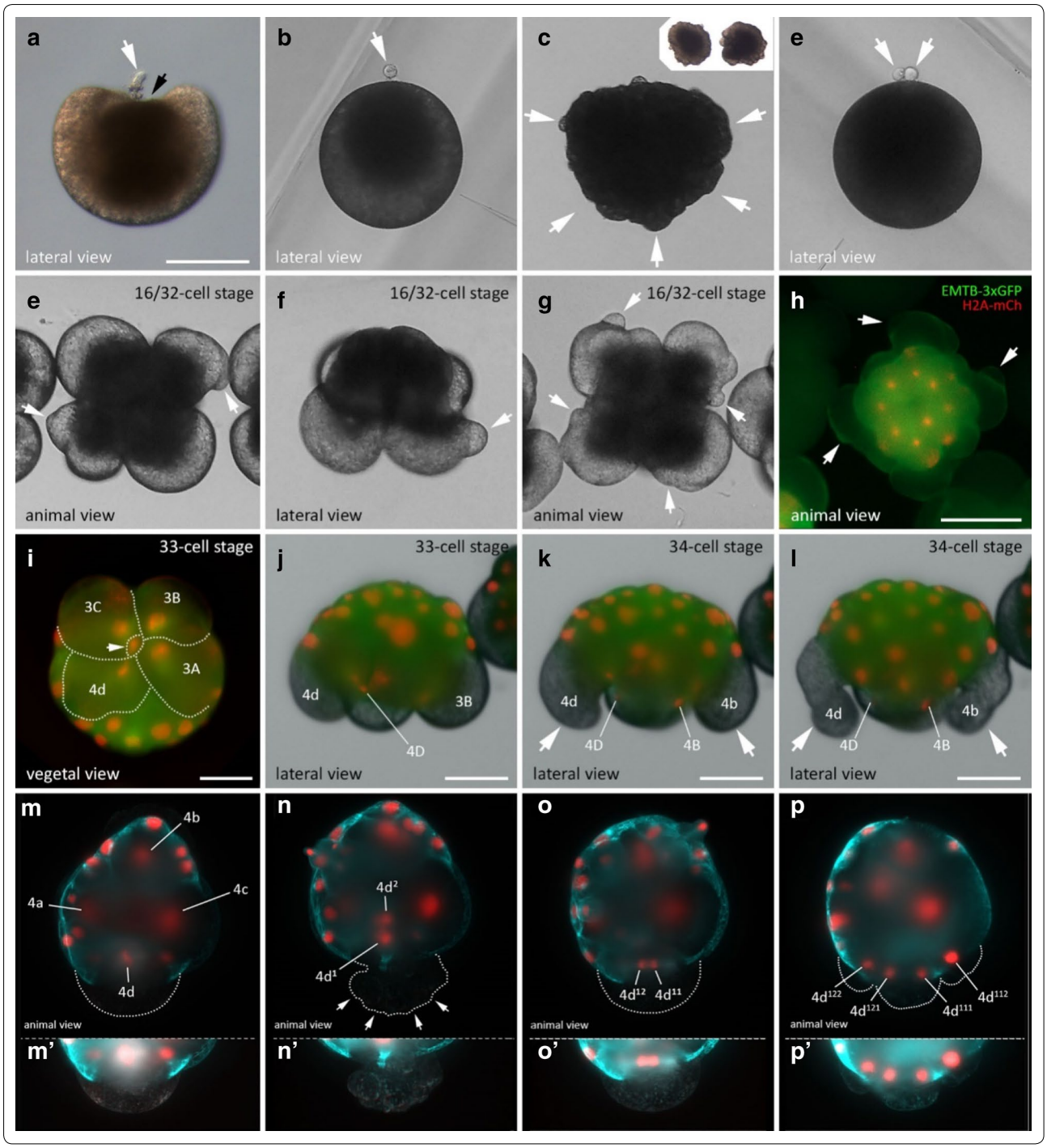

(Fig. 7m–p, m′–p′); $n = 16/16$). We can discard the possibility that cell blebbing is an artefact of removing the embryos from the egg shell or the agarose mounting procedure, because (a) we observed cell blebbing in embryos that were not embedded in agarose and imaged with an epifluorescence microscope (Fig. 7a–l), (b) cell blebbing was observed when following embryos that were still within the egg shell (personal observations), as has been also observed by Teshirogi et al. [72].

The perturbations of micromere 4d allow us to identify this cell even under a dissecting microscope without fluorescently labelled cells and to mark the end of a series of cell shape changes visible throughout early development. In Fig. 8, we summarize the events previously described

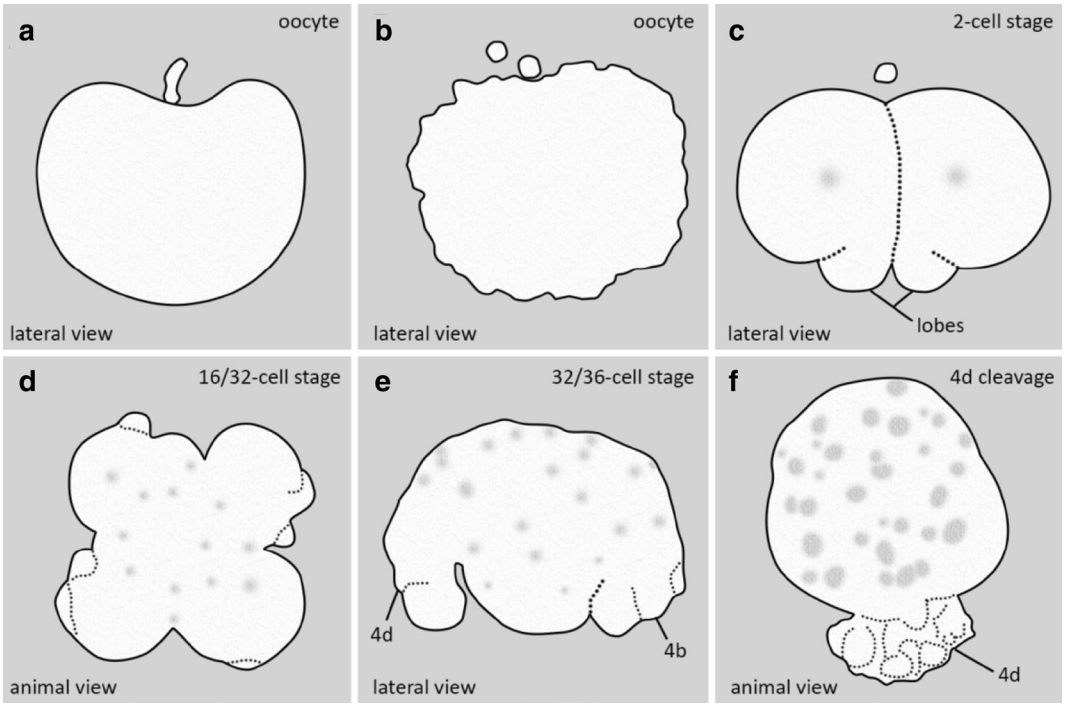

Fig. 8 Summary of cytoplasmic perturbations described in different polyclad flatworm species. **a** Depressions of the animal pole during the formation of the first polar body as described by Kato [35] for some Japanese polyclad species and observed for *Maritigrella crozieri* (this study) are shown. **b** Cell blebbing depicted in oocytes as described for most polyclads during the first and second meiotic divisions (see [19]. **c** Vegetal lobe like structures are shown found in *Pseudostylochus intermedius* [72] and *Pseudoceros japonicus* [48]. Schematic drawing was taken from *P. intermedius*. **d** Cytoplasmic perturbations as seen in *Pseudostylochus intermedius* (8- to 16-cell stage) [72] and *M. crozieri* (16- to 32-cell stage, this study). **e** Waves of contractile activity in all four macromeres of *M. crozieri* (this study) whereby macromeres attain an elongated shape. **f** Similar cytoplasmic perturbations seen during the highly asymmetric cleavage of micromere 4d found in *M. crozieri* (this study)

in polyclad flatworms, together with our own observations of the early development of *M. crozieri.*

It is interesting to see that the perturbations observed in *M. crozieri* during divisions of macromeres 2A–2D (extracellular vesicle-like structures; see Fig. 7e–h) look identical to a highly similar blebbing event in another polyclad species, the acotylean *Pseudostylochus intermedius* [72], although in the latter species, this phenomenon is described to take place one division round earlier (8- to 16-cell stage). Blebbing during the divisions of macromeres 3A–3D and the division of micromere 4d are both described by us for the first time during polyclad embryogenesis.

One observation suggesting that blebbing has an important function during polyclad embryogenesis is that when we mounted embryos in high concentrations of agarose (> 0.6%) we observed severely abnormal development ($n = 5/5$). We speculate that these defects may be caused by blebbing being hampered by the stiff agarose. Common to all of the blebbing events is that they are most visible in cells which contain lots of yolk and which undergo asymmetric divisions. Additionally, we show here that they coincide with increased cytoskeletal activity (mitosis). Ultimately, blebbing is the visible manifestation of actomyosin contractions of the cortex during strong cytoskeletal movements, which are more pronounced during asymmetric cleavages and in yolk-rich blastomeres.

Conclusions

In this study, we have used live imaging recordings and 3D reconstructions to extend observations of early development in a cotylean polyclad flatworm, *M. crozieri*. 3D reconstructions and continuous 4D recordings allow us to see developmental events in more detail than previously possible. We have been able to look at connections between nuclear movements and cell divisions and link them with cellular dynamics such as cell blebbing (protrusions of the membrane), and pinpoint important developmental events like symmetry breaking. Our observations allow us to confirm and extend previous developmental observations of early embryogenesis in polyclads, made using fixed specimens, describing the spiral cleavage pattern and the formation of the four

quartets. There seems to be little variation within both polyclad suborders, the cotyleans and the acotyleans.

One important observation in *M. crozieri* is that this so-called equal cleaving polyclad should probably be classified as such with caution. Our measurements of individual blastomeres at the four-cell stage show that the second cleavage is a product of unequal divisions of which one vegetal cross-furrow blastomere retains the largest volume. Similar observations of asymmetric cleavages may be a broader pattern within polyclads [77], but requires precise measurements to be carried out in different species. In *M. crozieri*, the question remains as to whether the observed size differences at the four-cell stage truly reflect an unequal cleavage mechanism, meaning that the D quadrant is already specified by maternal determinants at this early stage. Clearly, we need to know more about the molecular basis of putative maternal determinants and the mechanisms by which they could be sequestered. The sequestering of specific determinants, at least, seems to be supported by previous studies on *Hoploplana inquilina* [5, 6], however, evidence has also been found for inductive interactions between the first micromere quartet with other blastomeres [6]. The latter clearly resembles the equal cleavage mechanism found in canonical spiralian development and in this case the first two asymmetric cleavages could simply bias the resulting largest blastomere to produce descendants that are more likely to interact with the first quartet of micromeres. At present, neither an equal nor an unequal cleavage mechanism can be excluded.

Most importantly, we found that the animal–vegetal division of micromere 4d is present in both polyclad suborders, and we suggest this is a conserved pattern across all polyclad flatworms. It would be highly interesting to reinvestigate this cleavage pattern within the Prorhynchida, where the spiral cleavage pattern with quartet formation has also been partly retained but current developmental data are insufficient to conclude whether it follows the pattern as suggested for polyclads in this study.

We consider that the exact fate of both daughter cells of micromere 4d must be investigated more thoroughly before we can conclude whether micromere $4d^2$(animally positioned relative to $4d^1$) indeed represents the mesentoblast or not. Currently, even the fate of $4d^1$, despite its large size and the fact that it is readily visible at the onset of gastrulation, remains unclear, as model lineage tracing of this specific blastomere has not been yet performed. This could be done by DiI injections or perhaps via fluorescently tagged and photoconvertible molecules. It would also be interesting to study further the potential interaction of one of the daughter cells $4d^1$ with fourth quartet macromeres (4A–D), observed during our live imaging recordings in *M. crozieri*, and to find out whether there is any developmental role that can be assigned to the fourth quartet macromeres at later stages.

Our new data show that, in *M. crozieri*, blebbing is present not only in oocytes during meiosis, but also in macromeres during quartet formation and in micromere 4d during its first cleavage along the animal–vegetal axis (Figs. 6, 7 and Additional file 6). This must be a manifestation of the mechanical forces created by cytoskeletal dynamics during early cleavages, which may be more or less obvious depending on the polyclad species and perhaps the amount of yolk within the blastomere.

Taken together, the most crucial events during polyclad spiral cleavage take place as follows: After the first two cleavages one of the four blastomeres is slightly larger and typically is one of the two vegetal cross-furrow cells. At this point, the D quadrant might be already established by cytoplasmic localizations [6] but it is also possible that slight differences in size bias the largest blastomere of the four-cell stage to undergo D quadrant specification at a later stage via an inductive interaction (equal cleavage). The atypical formation of the fourth quartet gives rise to micromere 4d, which van den Biggelaar [74] suggested behaves in polyclads similarly to macromere 3D in molluscan and annelid embryos, insofar as 3D gives rise to the mesentoblast (4d). The formation of the mesentoblast in polyclads could therefore be delayed by at least one cell division. Unusually, micromere 4d undergoes an animal–vegetal division, which buds micromere $4d^2$ into the interior of the embryo and in proximity to the animal cap as shown by Surface [71] in *H. inquilina* and *M. crozieri* (this study). In our opinion the position that $4d^2$ assumes during this event would allow it to interact with micromeres of the first quartet. Such animal–vegetal inductive interactions are typically observed in equally cleaving spiralians during D quadrant specification [47], but would be delayed in polyclad flatworms. Ultimately, $4d^2$ may be considered the mesentoblast [15, 50], but this still remains to be determined more carefully.

As shown previously and in this work, polyclad flatworms appear to combine conserved features of spiral cleavage but also show obvious modifications of their cleavage program. This makes them a highly interesting taxon for evolutionary comparisons among flatworms within and outside the polyclad order but also across lophotrochozoan phyla. Live imaging recordings such as SPIM can certainly contribute also in future studies to extend our current understanding of polyclad development and of other marine invertebrates.

Methods

Animal culture

Adult specimens of *M. crozieri* were collected in coastal mangrove areas in the Lower Florida Keys, USA, in January 2014, November 2014, September 2015, and January 2016 near Mote Marine Laboratory (Latitude 24.661621, Longitude −81.454496). Animals were found on the ascidian *Ecteinascidia turbinata* as previously described [44]. Eggs without egg shells (to produce 'naked' embryos) were obtained from adults by poking with a needle (BD Microlance 3) and raised in Petri dishes coated with 2% agarose (diluted in filtered artificial seawater) or gelatin coated Petri dishes at room temperature in penicillin–streptomycin (100 µg/ml penicillin; 200 µg/ml streptomycin) treated Millipore filtered artificial seawater (35–36‰).

In vitro synthesis of mRNA

We synthesized mRNAs for microinjections with Ambion's SP6 mMESSAGEmMACHINE kit. The capped mRNAs produced were diluted in nuclease-free water and used for microinjections in order to detect fluorescence signal in early *M. crozieri* embryos. Nuclei were marked and followed using histone H2A-mCherry (H2A-mCh) and GFP-Histone (H2B-GFP). The plasmids carrying the nuclear marker pCS2-H2B-GFP (GFP-Histone) and pDestTol2pA2-H2A-mCherry [37] were transformed, purified and concentrated as described before and then linearized with the restriction enzymes NotI and BglII, respectively. To follow live microtubules, we used a GFP fusion of the microtubule binding domain of ensconsin (EMTB-3XGFP). These clones were the gift of the Bement Lab (University of Wisconsin) [8, 56] and were commercially ordered from http://addgene.org (EMTB-3XGFP: https://www.addgene.org/26741/).

Microinjections

Fine-tipped microinjection needles were pulled on a Sutter P-97 micropipette puller (parameters: $P=300$; $H=560$; $Pu=140$; $V=80$; $T=200$) and microinjections of synthesized mRNA (~300–400 ng/µl per mRNA in nuclease-free water) were carried out under a Leica DMI3000 B inverted scope with a Leica micromanipulator and a Picospitzer® III at room temperature.

4D microscopy of live embryos using OpenSPIM

Injected embryos ($n=15$) showing fluorescent signal were selected under an Axioimager M1 Epifluorescence and Brightfield Microscope (Zeiss). Live embryos were briefly incubated in 40 °C preheated and liquid low-melting agarose (0.1%) and immediately sucked into fluorinated ethylene propylene (FEP) tubes (Bola S1815-04), which were mounted in the OpenSPIM acquisition chamber which was filled with filtered artificial seawater and antibiotics via a 1-ml BD Plastikpak (REF 300013) syringe. The use of FEP tubes has been previously described [36] and allows the specimen to remain inside the tube during image acquisition without causing any blurring to the acquired images, as would be the case with other mounting materials such as glass capillaries. Using FEP tubes enables us to mount specimens in lower percentage agarose (0.1–0.2%), thus lessening the perturbation of embryo growth and development. Long-term imaging single timepointscan consist of 40–70 optical slices and were captured every 1–3 min. The OpenSPIM was assembled according to our previous description [20] and operated using MicroManager (version 1.4.19; November 7, 2014 release; https://www.micro-manager.org/).

4D microscopy of live embryos under an Axio Zoom.V16 (Zeiss)

Several embryos ($n=14$) in which fluorescent signal could be detected were centred within a 90 mm petri dish containing penicillin–streptomycin (100 µg/ml penicillin; 200 µg/ml streptomycin) treated Millipore filtered artificial seawater (35–36‰) for simultaneous live imaging. To avoid evaporation and make fluorescent imaging possible a tiny hole was made in the middle of the lid and artificial seawater containing fresh antibiotics carefully exchanged from the side when evaporation became apparent. Brightfield, green and red fluorescence was acquired every 5–7 min.

Fixation and imaging of embryos used for scanning electron microscopy (SEM)

Batches of embryos were raised until development reached the desired stage (1-cell, 2-cell, 4-cell, 8-cell, 16-cell, 32-cell, 64-cell and intermediate phases). Fixation was done at 4 °C for 1 h in 2.5% glutaraldehyde, buffered with phosphate buffered saline (PBS; 0.05 M PB/0.3 M NaCl, pH 7.2) and post-fixed at 4 °C for 20 min in 1% osmium tetroxide buffered with PBS. Fixed specimens were dehydrated in an ethanol series, dried via critical point drying, and subsequently sputtered coated with carbon or gold/palladium in a Gatan 681 high-resolution ion beam coater and examined with a Jeol 7401 high-resolution field emission scanning electron microscope (SEM).

Fixation and staining of embryos for 3D reconstruction

Embryos were extracted from gravid adults at the Keys Marine Laboratory (Florida) by poking and allowed to cleave until the desired stage was reached. Embryos were then fixed for 60 min in 4% formaldehyde (from 16% paraformaldehyde: 43368 EM Grade, AlfaAesar) in PBST

(0.1 M phosphate buffer saline containing 0.1% Tween 20) at room temperature, followed by a 5 × washing step in PBST and stored at 4 °C in PBST containing small concentrations of sodium azide.

In order to image specimens from five angles, which is necessary to perform volume measurements of early blastomeres, sodium azide with 0.1 M PBS containing 0.1% Triton X-100 in (PBSTx) was washed off fixed embryos by four washing steps and stained with 1:300 Rhodamine Phalloidin (ThermoFisher Scientific R415) for 2–3 h at room temperature or overnight at 4 °C. Following several washes of PBST or PBSTx 0.1 µM of the nuclear stain SytoxGreen (Invitrogen), which is difficult to detect at these early stages, was added for 30 min and the embryos then rinsed with PBST for another hour.

Volume measurements

The volume was measured manually in 3D reconstructed two- to four-cell stages ($n = 25$) using an open source Fiji-plugin (Volumest; http://lepo.it.da.ut.ee/~markkom/volumest/). Embryonic material came from pooled eggs extracted from various gravid animals, which were then allowed to develop until the desired stages were reached and then fixed as described above.

Image processing

Post-processing of acquired data was performed with the latest version of the freely available imaging software Fiji [68] and digital images were assembled in Adobe Photoshop CC 2017.

Additional files

Additional file 1. 50 min OpenSPIM movie of the third cleavage in an embryo of *M. crozieri* with labeld nuclei (H2B: GFP) showing spiral deformations (SD) and dexiotropic cleavage.

Additional file 2. Putative cell–cell interactions captured with an OpenSPIM of an embryo undergoing epiboly. It can be observed how nuclei of the fourth quartet macromeres (4A–4D) get in very close proximity with nuclei of close descendants of micromere $4d^1$ for a short period of time, which then goes away.

Additional file 3. An example of volume measurements performed on a four-cell stage polyclad flatworm embryo, showing only 5 representative slices within a Z-stack (the original file contains hundreds of slices after image processing is completed).

Additional file 4. Table of blastomere volume measurements in 2-, 3- and 4-cell stages. Vol.1 indicates the largest blastomere. In two-cell stages Vol.2 accounts for its sister cell. In four-cell stages Vol.2 corresponds to cells positioned clockwise (cw) of it, Vol. 3 to the cell opposite of it (opp) and Vol.4 counter clockwise (ccw) of it (see schematic embryo inset). The vegetal cross-furrow-cells (vcfc) are shown in orange.

Additional file 5. An average of the volume measurements of 3D reconstructed blastomeres in *M. crozieri* embryos of the 2-cell, 3-cell and 4-cell stages are shown. The data is based on measurements of individual blastomeres. To provide the data as percentages makes sense as each individual embryo can vary in size. The two-cell stages are indicated as blue columns (n = 13), three-cell stages as orange (n = 2) and four-cell stages as green columns (n = 13). Volumes are given as a percentage of the total volume of the embryo which is 100%. Standard deviations are indicated for smaller blastomeres only. In two-cell stages a 6% difference was noted between the two cells on average. The larger blastomere has been designated as CD. In three-cell stages the two sister blastomeres (C and D) have a larger volume than the remaining sister cell and have been designated as C and D according to a slight volume difference. In four-cell stages the largest blastomere is one of the vegetal cross-furrow cells and has been indicated as D. It is 5.8% larger compared to its sister cell indicated as C. Of the two, remaining sister blastomeres, the size difference is only 3.3% with the larger one indicated as blastomere B. Error bars indicate standard error of the mean.

Additional file 6. The initial division pattern of micromere 4d is shown using live imaging data from an Axio Zoom.V16 (Zeiss). The 4d blastomere does not divide laterally but first divides along the animal–vegetal axis into a smaller, animally positioned cell, which we designate as $4d^2$ and a larger, vegetally positioned cell, we designate as $4d^1$.

Additional file 7. Cytoplasmic perturbations were imaged with the OpenSPIM in one of the second quartet macromeres during mitosis. On the left the whole embryo is shown with increased brightness to visualize the membranous outlines of the macromeres better. To the right of each embryo, the nuclei of the same embryo are depicted with normal brightness levels. Red arrows point to the same nucleus of the embryo. A red line highlights the outline of the corresponding macromere. The shape deformations caused by the cytoplasmic perturbations of the macromere correlate precisely with the mitotic anaphase and reach a maximum in panel D. Scale bar = 50 µm.

Additional file 8. A movie of an embryo forming the third quartet. Prior to the cleavage of macromeres 2A–2D, blebbing becomes visible on the cell surfaces in form of small, vesicle-like protrusions. The movie shows that mitotic cytoskeletal activity during anaphase correlates with the observed protrusions.

Additional file 9. **(A-P)** A time-lapse recording showing the formation of the fourth quartet macromeres (4Q) and large micromeres (4q) of a single *M. crozieri* embryo in 5 min intervals with striking cytoplasmic perturbation activity at the vegetal pole of the embryo (indicated by black arrows). **(F-K)** 25 min of cytoplasmic perturbations are clearly visible in macromeres 3A–3D. Live imaging was performed under a Zeiss Axio Zoom. V16 Stereo Microscope. Scale bar is 100 µm.

Abbreviations

FEP: fluorinated ethylene propylene; MTOC: microtubule organizing centre; SEM: scanning electron microscopy; SPIM: selective plane illumination microscopy; SD: spiral deformations; PBS: phosphate-buffered saline.

Acknowledgements

We thank Anne Zakrzewski for her help with scanning electron microscopy pictures, Bernhard Egger and Kate Rawlinson for their continuous support and helpful discussions, Fraser Simpson for his immense effort during the Florida collection trips, the Mote Marine Laboratory (https://mote.org/) and Keys Marine Laboratory (http://www.keysmarinelab.org/) for their support during our stay in the Florida Keys.

Authors' contributions

MJT and JG designed the experiments. JG performed all the experiments and prepared the figures. JG and MJT analysed the data and wrote the manuscript. Both authors read and approved the final manuscript.

Funding

JG was funded by the Marie Curie ITN 'NEPTUNE' Grant (No. 317172), under the FP7 of the European Commission. M.J.T. was supported by the European Research Council (ERC-2012-AdG 322790), the Biotechnology and Biological Sciences Research Council grant (BB/H006966/1 and a Royal Society Wolfson Research Merit Award.

Availability of data and materials
AThe datasets during and/or analysed during the current study available from the corresponding author on reasonable request.

Ethics approval and consent to participate
Not applicable.

Consent for publication
Not applicable.

Competing interests
The authors declare that they have no competing interests.

Author details
[1] Centre for Life's Origins and Evolution, Department of Genetics, Evolution and Environment, University College London, London WC1E 6BT, UK. [2] Max Planck Institute of Molecular Cell Biology and Genetics, Pfotenhauerstraße 108, 01307 Dresden, Germany.

Received: 29 March 2019 Accepted: 8 June 2019
Published online: 22 June 2019

References

1. Aguinaldo AMA, Turbeville JM, Linford LS, Rivera MC, Garey JR, Raff RA, Lake JA. Evidence for a clade of nematodes, arthropods and other moulting animals. Nature. 1997;387:489–93.
2. Anderson DT. The embyonic and laval development of the turbellarian *Notoplana australis* (Schmarda, 1859) (Polycladida: Leptoplanidae). Mar Freshw Res. 1977;28:303–10.
3. Arnolds WJA, van den Biggelaar JAM, Verdonk NH. Spatial aspects of cell interactions involved in the determination of dorsoventral polarity in equally cleaving gastropods and regulative abilities of their embryos, as studied by micromere deletions in *Lymnaea* and *Patella*. Wilhelm Roux's Arch Dev Biol. 1983;192:75–85.
4. Astrow S, Holton B, Weisblat D. Centrifugation redistributes factors determining cleavage patterns in leech embryos. Dev Biol. 1987;120:270–83.
5. Boyer BC. Development of in vitro fertilized embryos of the polyclad flatworm, *Hoploplana inquilina*, following blastomere separation and deletion. Roux's Arch Dev Biol. 1987;196:158–64.
6. Boyer BC. The role of the first quartet micromeres in the development of the polyclad *Hoploplana inquilina*. Biol Bull. 1989;177:338–43.
7. Boyer BC, Henry JQ, Martindale MQ. The cell lineage of a polyclad turbellarian embryo reveals close similarity to coelomate spiralians. Dev Biol. 1998;204:111–23.
8. Burkel BM, Von Dassow G, Bement WM. Versatile fluorescent probes for actin filaments based on the actin-binding domain of Utrophin. Cell Motil Cytoskelet. 2007;64:822–32.
9. Cather JN, Verdonk NH. Development of *Dentalium* following removal of D-quadrant blastomeres at successive cleavage stages. Wilhelm Roux's Arch Dev Biol. 1979;187:355–66.
10. Clement AC. Experimental studies on germinal localization in Ilyanassa. I. The role of the polar lobe in determination of the cleavage pattern and its influence in later development. J Exp Zool. 1952;121:593–625.
11. Clement AC. Development of Ilyanassa following removal of the D macromere at successive cleavage stages. J Exp Zool. 1962;149:193–215.
12. Cowan CR, Hyman AA. Asymmetric cell divisions in *C. elegans*: cortical polarity and spindle positioning. Annu Rev Cell Dev Biol. 2004;20:427–53.
13. Dorresteijn AWC, Bornewasser H, Fischer A. A correlative study of experimentally changed first cleavage and Janus development in the trunk of *Platynereis dumerilii* (Annelida, Polychaeta). Roux's Arch Dev Biol. 1987;196:51–8.
14. Dunn CW, Hejnol A, Matus DQ, Pang K, Browne WE, Smith SA, Seaver E, Rouse GW, Obst M, Edgecombe GD, Sørensen MV, Haddock SHD, Schmidt-Rhaesa A, Okusu A, Kristensen RM, Wheeler WC, Martindale MQ, Giribet G. Broad phylogenomic sampling improves resolution of the animal tree of life. Nature. 2008;452:745–9.
15. Egger B, Lapraz F, Tomiczek B, Müller S, Dessimoz C, Girstmair J, Škunca N, Rawlinson KA, Cameron CB, Beli E, Todaro MA, Gammoudi M, Noreña C, Telford MJ. A transcriptomic–phylogenomic analysis of the evolutionary relationships of flatworms. Curr Biol. 2015;25:1347–53.
16. Freeman G, Lundelius WJ. Evolutionary implications of the mode of D quadrant specification in coelomates with spiral cleavage. J Evol Biol. 1992;5:205–47.
17. Friedrich HH. Morphogenese der Tiere. Handbuch der ontogenetischen Morphologie und Physiologie in Einzeldarstellungen. Herausgegeben von Friedrich Seidel., Reihe I: Deskriptive Morphogenese, Lief. 3: D5-I. Hermann Friedrich: Nemertini. *Gustav Fischer Verlag, Stuttgart*; 1979, p. 1–169.
18. Gammoudi M, Noreña C, Tekaya S, Prantl V, Egger B. Insemination and embryonic development of some Mediterranean polyclad flatworms. Invertebr Reprod Dev. 2011;56:272–86.
19. Gammoudi M, Egger B, Tekaya S, Noreña C. The genus *Leptoplana* (Leptoplanidae, Polycladida) in the Mediterranean basin. Redescription of the species *Leptoplana mediterranea* (Bock, 1913) comb. nov. Zootaxa. 2012;56:45–56.
20. Girstmair J, Zakrzewski A, Lapraz F, Handberg-thorsager M, Tomancak P, Pitrone PG, Simpson F, Telford MJ. Light-sheet microscopy for everyone? Experience of building an OpenSPIM to study flatworm development. BMC Dev Biol. 2016;16:1–16.
21. Goette A. Zur Entwicklungsgeschichte der Würmer. Zool Anz. 1881;4:189–91.
22. Gualda EJ, Vale T, Almada P, Feijó JA, Martins GG, Moreno N. OpenSpinMicroscopy: an open-source integrated microscopy platform. Nat Methods. 2013;10:599–600.
23. Halanych KM, Bacheller JD, Aguinaldo AM, Liva SM, Hillis DM, Lake JA. Evidence from 18S ribosomal DNA that the lophophorates are protostome animals. Science (80-). 1995;267:1641–3.
24. Hallez PP. Contributions à l'histoire naturelle des Turbellariés. Trav l'Institut Zool Lille la Stn Marit Wimereux. 1879;2:1–213.
25. Hartenstein V, Ehlers U. The embryonic development of the rhabdocoel flatworm *Mesostoma lingua* (Abildgaard, 1789). Dev Genes Evol. 2000;210:399–415.
26. Hejnol A. A twist in time-the evolution of spiral cleavage in the light of animal phylogeny. Integr Comp Biol. 2010;50:695–706.
27. Hejnol A, Obst M, Stamatakis A, Ott M, Rouse GW, Edgecombe GD, Martinez P, Baguñà J, Bailly X, Jondelius U, Wiens M, Müller WEG, Seaver E, Wheeler WC, Martindale MQ, Giribet G, Dunn CW. Assessing the root of bilaterian animals with scalable phylogenomic methods. Proc R Soc B Biol Sci. 2009;276:4261–70.
28. Henry JJ. The role of unequal cleavage and the polar lobe in the segregation of developmental potential during first cleavage in the embryo of *Chætopterus variopedatus*. Roux's Arch Dev Biol. 1986;195:103–16.
29. Henry JJ. Removal of the polar lobe leads to the formation of functionally deficient photocytes in the annelid Chætopterus variopedatus. Roux's Arch Dev Biol. 1989;198:129–36.
30. Henry JQ. Spiralian model systems. Int J Dev Biol. 2014;58:389–401.
31. Henry JJ, Martindale MQ. The organizing role of the D quadrant as revealed through the phenomenon of twinning in the polycheate *Chætopterus variopedatus*. Roux's Arch Dev Biol. 1987;196:499–510.
32. Henry JQ, Martindale MQ. Conservation of the spiralian developmental program: cell lineage of the nemertean, *Cerebratulus lacteus*. Dev Biol. 1998;201:253–69.
33. Henry JJ, Martindale MQ. Conservation and innovation in spiralian development. Hydrobiologia. 1999;402:255–65.
34. Henry JQ, Perry KJ, Martindale MQ. Cell specification and the role of the polar lobe in the gastropod mollusc *Crepidula fornicata*. Dev Biol. 2006;297:295–307.
35. Kato K. On the development of some Japanese polyclads. Jpn J Zool. 1940;8:537–74.
36. Kaufmann A, Mickoleit M, Weber M, Huisken J. Multilayer mounting enables long-term imaging of zebrafish development in a light sheet microscope. Development. 2012;139:3242–7.
37. Kwan KM, Fujimoto E, Grabher C, Mangum BD, Hardy ME, Campbell DS, Parant JM, Yost HJ, Kanki JP, Chien C-B. The Tol2kit: a multisite gateway-based construction kit for Tol2 transposon transgenesis constructs. Dev Dyn. 2007;236:3088–99.
38. Lambert JD. Mesoderm in spiralians: the organizer and the 4d cell. J Exp Zool Part B Mol Dev Evol. 2008;310:15–23.
39. Lambert JD. Patterning the spiralian embryo: insights from *Ilyanassa*. In *Current topics in developmental biology*. 2009, p. 107–133. Elsevier Inc.

40. Lambert JD. Developmental patterns in spiralian embryos. Curr Biol. 2010;20:R72–7.
41. Lambert JD, Nagy LM. MAPK signaling by the D quadrant embryonic organizer of the mollusc *Ilyanassa obsoleta*. Development. 2001;128:45–56.
42. Lambert JD, Nagy LM. The MAPK cascade in equally cleaving spiralian embryos. Dev Biol. 2003;263:231–41.
43. Lang A. Die Polycladen (Seeplanarien) des Golfes von Neapel: und der angrenzenden Meeres-Abschnitte: eine Monographie. Leipzig: Leipzig, Verlag von Wilhelm Engelmann; 1884.
44. Lapraz F, Rawlinson KA, Girstmair J, Tomiczek B, Berger J, Jékely G, Telford MJ, Egger B. Put a tiger in your tank: the polyclad flatworm *Maritigrella crozieri* as a proposed model for evo-devo. Evodevo. 2013;4:1–15.
45. Lehmann FE, Hadorn H. Vergleichende Wirkungsanalyse von zwei antimitotischen Stoffen, Colchicin und Benzochinon, am Tubifex-Ei. Helv Physiol Pharmacol Acta. 1946;4:11–42.
46. Li R, Albertini DF. The road to maturation: somatic cell interaction and self-organization of the mammalian oocyte. Nat Rev Mol Cell Biol. 2013;14:141–52.
47. Lyons DC, Henry JQ. Ins and outs of spiralian gastrulation. Int J Dev Biol. 2014;58:413–28.
48. Malakhov VV, Trubitsina NV. Embryonic development of the polyclad turbellarian *Pseudoceros japonicus* from the sea of Japan. Russ J Mar Biol. 1998;24:106–13.
49. Marlétaz F, Peijnenburg KTCA, Goto T, Satoh N, Rokhsar DS. A new spiralian phylogeny places the enigmatic arrow worms among gnathiferans. Curr Biol. 2019;29:312–8.
50. Martín-Durán JM, Egger B. Developmental diversity in free-living flatworms. Evodevo. 2012;3:1–22.
51. Martindale MQ. The 'organizing' role of the D quadrant in an equal-cleaving spiralian, *Lymnaea stagnalis* as studied by UV laser deletion of macromeres at intervals between third and fourth quartet formation. Int J Invertebr Reprod Dev. 1986;9:229–42.
52. Martindale MQ, Doe CQ, Morrill JB. The role of animal-vegetal interaction with respect to the determination of dorsoventral polarity in the equal-cleaving spiralian, *Lymnaea palustris*. Wilhelm Roux's Arch Dev Biol. 1985;194:281–95.
53. Maslakova SA, Martindale MQ, Norenburg JL. Fundamental properties of the spiralian developmental program are displayed by the basal nemertean *Carinoma tremaphoros* (Palaeonemertea, Nemertea). Dev Biol. 2004;267:342–60.
54. Meshcheryakov V. The common pond snail *Lymnaea stagnalis*. In: Dettlaff T, Vassetzky S, editors. Animal species for developmental studies Volume 1 Invertebrates. 1st ed. Moscow: Springer; 1991. p. 69–131.
55. Meyer NP, Boyle MJ, Martindale MQ, Seaver EC. A comprehensive fate map by intracellular injection of identified blastomeres in the marine polychaete *Capitella teleta*. Evodevo. 2010;1:8.
56. Miller AL, Bement WM. Regulation of cytokinesis by Rho GTPase flux. Nat Cell Biol. 2009;11:71–7.
57. Morris J, Nallur R, Ladurner P, Egger B, Rieger R, Hartenstein V. The embryonic development of the flatworm *Macrostomum* sp. Dev Genes Evol. 2004;214:220–39.
58. Nakama AB, Chou HC, Schneider SQ. The asymmetric cell division machinery in the spiral-cleaving egg and embryo of the marine annelid *Platynereis dumerilii*. BMC Dev Biol. 2017;17:1–22.
59. Pick KS, Philippe H, Schreiber F, Erpenbeck D, Jackson DJ, Wrede P, Wiens M, Alié A, Morgenstern B, Manuel M, Wörheide G. Improved phylogenomic taxon sampling noticeably affects nonbilaterian relationships. Mol Biol Evol. 2010;27:1983–7.
60. Pitrone PG, Schindelin J, Stuyvenberg L, Preibisch S, Weber M, Eliceiri KW, Huisken J, Tomancak P. OpenSPIM—an open access platform for light sheet microscopy. Nat Methods. 2013;10:598–9.
61. Rawlinson KA. Embryonic and post-embryonic development of the polyclad flatworm *Maritigrella crozieri*; implications for the evolution of spiralian life history traits. Front Zool. 2010;7:1–25.
62. Rawlinson KA. The diversity, development and evolution of polyclad flatworm larvae. Evodevo. 2014;5:1–12.
63. Rawlinson KA, Marcela Bolaños D, Liana MK, Litvaitis MK. Reproduction, development and parental care in two direct-developing flatworms (Platyhelminthes: Polycladida: Acotylea). J Nat Hist. 2008;42:2173–92.
64. Ren X, Weisblat DA. Asymmetrization of first cleavage by transient disassembly of one spindle pole aster in the leech *Helobdella robusta*. Dev Biol. 2006;292(1):103–15.
65. Render JA. The second polar lobe of the *Sabellaria cementarium* embryo plays an inhibitory role in apical tuft formation. Wilhelm Roux's Arch Dev Biol. 1983;192:120–9.
66. Render JA. Development of *Ilyanassa obsoleta* embryos after equal distribution of polar lobe material at first cleavage. Dev Biol. 1989;132:241–50.
67. Rice ME. Sipuncula: developmental evidence for phylogenetic inference. In: Morris SC, George JD, Gibson R, Platt HM, editors. The origins and relationships of lower invertebrates. Oxford: Oxford University Press; 1985. p. 274–96.
68. Schindelin J, Arganda-Carreras I, Frise E, Kaynig V, Longair M, Pietzsch T, Preibisch S, Rueden C, Saalfeld S, Schmid B, Tinevez J-Y, White DJ, Hartenstein V, Eliceiri K, Tomancak P, Cardona A. Fiji—an Open Source platform for biological image analysis. Nat Methods. 2012;9:676–82.
69. Selenka E.. Zoologische Studien II. Zur Entwickelungsgeschichte der Seeplanarien. Leipzig; 1881.
70. Shibazaki Y, Shimizu M, Kuroda R. Body handedness is directed by genetically determined cytoskeletal dynamics in the early embryo. Curr Biol. 2004;14:1462–7.
71. Surface FM. The early development of a polyclad, *Planocera inquilina*. Proc Acad Natl Sci Phila. 1907;59:514–59.
72. Teshirogi W, Sachiko I, Jatani K. On the early development of some Japanese polyclads. Rep Fukaura Mar Biol Lab. 1981;9:2–31.
73. van den Biggelaar JAM. Development of dorsoventral polarity and mesentoblast determination in *Patella vulgata*. J Morphol. 1977;154:157–86.
74. van den Biggelaar JAM. Cleavage pattern and mesentoblast formation in *Acanthochiton crinitus* (Polyplacophora, Mollusca). Dev Biol. 1996;174:423–30.
75. van den Biggelaar JAM, Guerrier P. Dorsoventral polarity and mesentoblast determination as concomitant results of cellular interactions in the mollusk *Patella vulgata*. Dev Biol. 1979;68:462–71.
76. Van den Biggelaar JAM, Guerrier P. Origin of spatial organization. In: Wilbur KM, editor. The Mollusca. CA: San Diego; 1983.
77. van den Biggelaar JAM, Dictus WJAG, van Loon AE. Cleavage patterns, cell-lineages and cell specification are clues to phyletic lineages in Spiralia. Sem Cell Dev Biol. 1997;8(4):367–78.
78. Verdonk NH, Van den Biggelaar JAM. Early development and the formation of the germ layers. In: Wilbur KM, editor. The Mollusca. 3rd ed. CA: San Diego; 1983. p. 91–122.
79. Wall R. From oocyte to zygote. In: Barlow PW, Bray D, Green PB, Slack JMW, editors. This side up—spatial determination in the early development of animals. Cambridge: Cambridge University Press; 1990. p. 31–45.
80. Wierzejski A. Embryologie von *Physa fontinalis* L. Zeitschrift für wissenschaftliche Zool. 1905;83:502–706.
81. Willems M, Egger B, Wolff C, Mouton S, Houthoofd W, Fonderie P, Couvreur M, Artois T, Borgonie G. Embryonic origins of hull cells in the flatworm *Macrostomum lignano* through cell lineage analysis: developmental and phylogenetic implications. Dev Genes Evol. 2009;219:409–17.
82. Wilson EB. Considerations on cell-lineage and ancestral reminiscence, based on a re-examination of some points in the early development of annelids and polyclades. Ann N Y Acad Sci. 1898;11:1–27.
83. Younossi-Hartenstein A, Hartenstein V. The embryonic development of the polyclad flatworm *Imogine mcgrathi*. Dev Genes Evol. 2000;210:383–98.

Publisher's Note